Evaluating surfactant effectiveness in preventing antibody adsorption directly on medical surfaces using a novel device

Rosa Álvarez-Palencia Jiménez, Antoine Maze, Franz Bruckert, Fethi Bensaid, Naila El-Kechai, Marianne Weidenhaupt

European Journal of Pharmaceutics and Biopharmaceutics 205 (2024) 114539

Contents lists available at ScienceDirect

European Journal of Pharmaceutics and Biopharmaceutics

journal homepage: www.elsevier.com/locate/ejpb

Evaluating surfactant effectiveness in preventing antibody adsorption directly on medical surfaces using a novel device

Rosa Álvarez-Palencia Jiménez [a,b], Antoine Maze [a], Franz Bruckert [a], Fethi Bensaid [c], Naila El-Kechai [b], Marianne Weidenhaupt [a,*]

[a] Univ. Grenoble Alpes, CNRS, Grenoble INP* (*Institute of Engineering) LMGP, 38000 Grenoble, France
[b] Sanofi, 94400 Vitry-sur-Seine, France
[c] Sanofi, 69280 Marcy-L'Etoile, France

ARTICLE INFO

Keywords:
Monoclonal Antibody
Antibody-Drug Conjugate
Surfactant
Adsorption
IV Bag
Manufacturing Bag
ELISA
Formulation
In-Use Stability

ABSTRACT

Biopharmaceuticals, specifically antibody-based therapeutics, have revolutionized disease treatment. Throughout their lifecycle, these therapeutic proteins are exposed to several stress conditions, for example at interfaces, posing a risk to the drug product stability, safety and quality. Therapeutic protein adsorption at interfaces may lead to loss of active product and protein aggregation, with potential immunogenicity risks. Non-ionic surfactants are commonly added in formulations to mitigate protein-surface interactions. However, their effectiveness varies with the monoclonal antibody (mAb), and model surface material. Extrapolating findings from model surfaces to real medical surfaces is challenging due to diverse properties.

This study pioneers the evaluation of surfactant effectiveness in preventing mAb adsorption directly on medical surfaces at the medical bag/formulation interface, utilizing the ELIBAG device. The adsorption of different protein modalities, mAbs and antibody-drug conjugate (ADC), using three surfactants (PS80, PS20, and P188), was examined across various medical surfaces, IV bags and manufacturing bags, and model surfaces. Our findings reveal that surfactants prevent mAb adsorption depending on the mAb modality, surfactant type and concentration, and surface material. This research underscores the importance of considering real medical surfaces in direct contact with formulations, offering insights for enhancing drug product development and ensuring material-protein compatibility in real world use.

1. Introduction

Biopharmaceuticals have emerged as important drugs for the treatment in several major disease areas, including oncology, immunology and chronic diseases [1,2]. Specifically, antibody-based biotherapeutics, such as monoclonal antibodies (mAbs) and antibody-drug conjugates (ADCs), are one of the fastest-growing segments within the pharmaceutical market since the last decades [3]. These therapeutic proteins are exposed to several stress conditions during their lifecycle, such as temperature, mechanical stress, and surface adsorption, that might lead to protein aggregation, posing a risk to the drug product stability, safety and quality [4]. Biopharmaceuticals are in contact with a variety of interfaces during drug product development, storage, and clinical administration (*e.g.*, manufacturing plastic bags, tubing, filter surfaces and intravenous (IV) administration bags) [5,6]. Given the amphiphilic properties of mAbs and the predominant hydrophobic nature of these medical surfaces, mAbs can adsorb at interfaces based on interactions between hydrophobic regions of the mAb and the material surface [6–8].

Protein adsorption to interfaces may lead to (1) a risk of mAb losses, and therefore a reduced dose of the active ingredient available for therapy, especially for low concentration drug products or after dilution [9,10], and (2) mAb structural changes and undesirable protein aggregates in solution, with potential immunogenic effects on patients [7,11]. Non-ionic surfactants are typically added in mAb-based formulations in order to reduce protein-surface interactions. Polysorbate 80 (PS80) and polysorbate 20 (PS20) are more commonly employed than poloxamer 188 (P188). The main mechanism of protein stabilization by non-ionic surfactants is by competition of surfactants and proteins at interfaces, where adsorbed surfactants can prevent protein adsorption and aggregation [12]. Best practices involve the addition of surfactants above their critical micelle concentration (CMC), however, the concentration often varies depending on the protein formulation [13]. In addition, it

* Corresponding author at: Phelma Minatec LMGP, 3 parvis Louis Neel, CS 50257, F-38016 Grenoble cedex 1, France.
E-mail address: marianne.weidenhaupt@grenoble-inp.fr (M. Weidenhaupt).

https://doi.org/10.1016/j.ejpb.2024.114539
Received 3 July 2024; Received in revised form 16 September 2024; Accepted 18 October 2024
Available online 20 October 2024

should be considered that when mAb-based products are administered via IV infusion, the formulations are diluted into the administration IV bags, thus decreasing the concentration of surfactants, and potentially their protective effect [14].

Although surfactants are known to prevent mAb adsorption at interfaces, previous investigations on model surfaces (*e.g.*, model plastic 96-well plates and/or functionalised sensors) have shown that their protection efficacy depends on the surface, surfactant, and mAb properties [15–17]. The molecular adsorption behaviour on such model surfaces might not fully represent the adsorption on real medical surfaces, considering that their surface composition can be complex and sometimes not fully characterized. They can be made of several layered polymers and contain additives for flexibility and transparency [18], the characteristics of which are difficult to fully mimic on model polymer surfaces and functionalised sensors.

Concerning model surfaces (commercially available 96-well plates), we have previously demonstrated that surfactant protection efficacy (PS80 at 200 ppm) to prevent mAb (30 mg/mL) adsorption depends on the hydrophobic plastic model surface. We found an intermediate efficacy on cyclic olefin copolymer (COC) and polyvinylchloride (PVC) surfaces, while PS80 exhibited a great efficacy in preventing mAb adsorption on polypropylene (PP), polystyrene (PS) and polycarbonate (PC) surfaces [16]. In addition, a recent study by Zürcher D *et al.* [17] has examined the protection efficacy of four surfactants (PS80, PS20, P188 and Brij 35) to prevent mAb adsorption by using a nanoparticle-based approach. They demonstrated that the four surfactants protect well at the air/liquid interface but exhibit different stabilizing effects at the solid/liquid interfaces depending on the surface.

Regarding real medical surfaces, in the biopharmaceutical industry, in-use studies are critical to investigate the compatibility between representative materials in direct contact with drug products. These studies are essentially focused on analytical methods to measure mAb stability in liquid solution [18]. Prior research highlighted the importance of investigating material – formulation compatibilities on medical containers, such as on polyolefin (PO) and PVC IV bags [9,19]. For example, mAb losses due to aggregate formation in PVC bags were higher than in PO bags [20]. However, there is a lack of studies evaluating the protection efficacy of surfactants at the solid/liquid interface directly on medical surfaces, which would be beneficial for material-protein compatibility investigations.

Recently, we have developed and optimized a device and protocol to detect and quantify mAb adsorption directly on medical plastic bags, ELIBAG [21]. The adsorption of mAb (in the absence of surfactant) was measured directly on a PP IV Administration Bag and a low-density polyethylene (LD-PE) Manufacturing Bag, showing a similar mAb bulk concentration range (0.01–0.1 mg/mL) for mAb surface saturation, both on medical bags and model surfaces (plastic 96-well plates).

In the present work, we focus on evaluating for the first time the surfactant efficacy to prevent pharmaceutical protein adsorption directly on medical surfaces at the medical surface/formulation interface, using the ELIBAG device, previously described [21]. We evaluated three protein pharmaceuticals, two mAbs and one ADC, in the presence or absence of the three surfactants PS80, PS20, and P188, at different concentrations. We have tested a variety of medical surfaces, such as IV administration bags and manufacturing pharmaceutical bags, made of different materials including PP, PVC, and LD-PE. Additionally, we characterized the material composition of model and medical plastic surfaces, highlighting potential correlations between material surface properties and the efficacy of surfactants in preventing protein adsorption. Overall, we have found that the protein adsorption levels depend on the protein modality, the type of surfactant and concentration, and the material in contact with the formulation. Furthermore, we show that the adsorption behaviour of mAbs and surfactants on model surfaces may not reflect the performance on real medical surfaces, even for similar surface composition. This is also the case for medical surfaces made of the same polymer from different suppliers.

Our multiparameter study allows to pinpoint differences in surfactant-mAb-container combinations that can guide formulation optimisation while addressing, at the same time, material compatibility. Previous studies have examined protein and surfactant adsorption using diverse techniques, setups, and model surfaces in various formats, thereby presenting challenges in directly comparing findings across investigations. Our methodology, facilitated by ELIBAG device, is well-suited for comparing real formulations in direct contact with medical surfaces. Through our comprehensive comparative study, we highlight key insights contributing to a deeper understanding of mAb adsorption to plastic surfaces. Thus, this research holds significant potential for drug product development, particularly in in-use studies, offering valuable tools for assessing pharmaceutical protein adsorption with various excipients on a range of medical plastic bags, from manufacturing to administration.

2. Materials & methods

2.1. Materials

2.1.1. Monoclonal antibody A (mAbA)

Monoclonal antibody A (mAbA) is an IgG1, provided by Sanofi (Paris, France) at 30 g/L in a formulation at pH 6.0 containing histidine and sucrose; mAbA is positively charged at pH 6.0. The buffer used for mAbA, named Bf1X Histidine/Sucrose, contains 10 % w/v Sucrose, L-Histidine and L-Histidine monohydrochloride monohydrate with a pH of 6.0. Concentrated mAbA was stored at −20 °C in 1 mL aliquots and thawed before each experiment. When thawed, mAbA was kept at 4 °C before dilution at the working concentration in the corresponding Bf1X Histidine/Sucrose. mAbA aliquot concentrations were confirmed by measuring absorbance at 280 nm using a Nanodrop 2000 (Thermo Fisher) spectrophotometer.

2.1.2. Monoclonal antibody N (mAbN)

Monoclonal antibody N (mAbN) is an IgG1, provided by Sanofi (Paris, France) at 27 g/L in 20 mM acetate with 5 % w/v sucrose buffer at pH 5.5. mAbN is positively charged at pH 5.5. The buffer used for mAbN, named Bf1X Acetate/Sucrose, contains Acetate sodium trihydrate, Acetic acid and Sucrose 5 % w/v, with a pH of 5.5. Concentrated mAbN was stored at −20 °C in 1 mL aliquots and thawed before each experiment. When thawed, mAbN was kept at 4 °C before dilution at the working concentration in the corresponding Bf1X Acetate/Sucrose. mAbN aliquot concentrations were confirmed by measuring absorbance at 280 nm using a Nanodrop 2000 (Thermo Fisher) spectrophotometer.

2.1.3. Antibody-Drug Conjugate (ADC)

The Antibody-Drug Conjugate (ADC) is an IgG1-type monoclonal antibody (mAbN) linked to a cytotoxic drug, provided by Sanofi (Paris, France) at 12.5 g/L in 10 mM acetate buffer with 5 % w/v sorbitol at pH 5.5; ADC is positively charged at pH 5.5. The buffer used for ADC, named Bf1X Acetate/Sorbitol, contains Acetate sodium trihydrate, Acetic acid and 5 % w/v Sorbitol, with a pH of 5.5. Concentrated ADC was stored at −20 °C in 1 mL aliquots and thawed before each experiment. When thawed, ADC was kept at 4 °C before dilution at the working concentration in the corresponding Bf1X Acetate/Sorbitol. ADC aliquot concentrations were confirmed by measuring absorbance at 280 nm using a Nanodrop 2000 (Thermo Fisher) spectrophotometer.

2.1.4. Secondary Protein: Protein G–HRP conjugate

Protein G-HRP (Merck 18–161) was rehydrated at 1 $g{\cdot}L^{-1}$ in MilliQ water. Concentrated protein aliquots were stored at − 20 °C and thawed prior to use. Upon thawing, PtG-HRP was prepared in dark bottles at 500 $\mu g{\cdot}L^{-1}$ in the corresponding Bf1X with 30 min agitation (stock solutions). Then, the required working concentrations were obtained by dilution of the stock solutions in Bf1X. PtG-HRP has an average molecular weight of 73 kDa, the HRP:PtG ratio is 1:1 (indicated by the

supplier), and there are 2 theoretical binding sites for PtG in the Fc fragment of the mAb in solution (given by the supplier).

2.1.5. Polysorbate 80 (PS80)

Super Refined™ Polysorbate 80 (PS80) (Croda, SR40925) was used and is compliant with EP, USP and JP monographs. PS80 has a molecular weight of 1310 g·mol^{-1}, a critical micellar concentration (CMC) of 0.016 mg/mL (16 ppm) (at 20–25 °C in water) and a hydrophilic-lipophilic-balance (HLB) of 15 [22]. Stock solutions of PS80 were prepared in dark bottles at 10000 ppm in the corresponding buffer (Bf1X) with 1 h agitation. This surfactant stock solution was covered by nitrogen gas and stored at 4 °C and remained viable for experiments for up to one month from the preparation date.

2.1.6. Polysorbate 20 (PS20)

Polysorbate 20 (PS20) (Seppic Montanox 20ppi, 820645) was used and is compliant with EP, USP and JP monographs. PS20 has a molecular weight of 1228 g·mol^{-1}, a CMC of 0.072 mg/mL (72 ppm) (at 20–25 °C in water) and a HLB of 16.7 [22]. Stock solutions of PS20 were prepared in dark bottles at 10000 ppm in the corresponding buffer (Bf1X) with 1 h agitation. This surfactant stock solution was covered by nitrogen gas and stored at 4 °C and remained viable for experiments for up to one month from the preparation date.

2.1.7. Poloxamer 188 (P188)

Poloxamer 188 (P188) (Emprove® Expert, Merck, 137112) was used and is compliant with EP, USP and JP monographs. P188 has a molecular weight of 8400 g.mol^{-1}, a CMC of 0.34 mg/mL (340 ppm) (at 20–25 °C in water) and a HLB of 29 [22]. Stock solutions of P188 were prepared in dark bottles at 10000 ppm in the corresponding buffer (Bf1X) with 1 h agitation. This surfactant stock solution was covered by nitrogen gas and stored at 4 °C and remained viable for experiments for up to one month from the preparation date.

2.1.8. Model plastic surfaces

Polystyrene and polypropylene 96-well microplates were purchased from Greiner (references 655101 and 650201, respectively) and polyvinylchloride 96-well microplates were purchased from Corning (reference 2595).

2.1.9. Model and medical plastic surfaces

The following model and medical plastic surfaces were investigated in the present study (Table 1). The main polymer surface composition of the inner surfaces of polyolefin (PO) bags was found to be polypropylene (PP) (detected by ATR-FTIR). The surface characterization is discussed in the section results and discussion. A summary of container category, type, supplier and reference, lot number of the bags, assigned name, and sterilization process is included in Table 1.

2.1.10. Direct Enzyme-Linked Immunosorbent Assay (ELISA)

To investigate antibody adsorption directly on medical surfaces, we developed an ELISA-based device from the initial design concept of combining the medical plastic bag, a bottom-less PS plate (Greiner Bio-One, reference 655000), and a holder to enclose the system, with the purpose of performing an ELISA test directly on the medical bag. This innovative device, named ELIBAG, is described in [21]. An adapted ELISA test, based on a previously established protocol [16], can be performed in the device to quantify the amount of antibody adsorbed directly on the medical surface. The adsorption of mAb on the plastic surface is detected via a secondary protein (PtG) coupled to a horseradish peroxidase enzyme (HRP).

Bags were cut open and placed in the ELIBAG device with the inner surface of the bags in contact with the mAb formulation. In the case of pre-filled bags, they were emptied prior to placing into the ELIBAG device. Comparative studies were conducted to assess mAbA adsorption and PS80 protection efficacy within both emptied bags and emptied bags that had been washed with water. Results indicated no significant difference between the two conditions of bags with and without washing before adsorption tests. Therefore, pre-filled bags were emptied and directly placed into the ELIBAG.

mAbA was used at 2 mg/mL diluted in Bf1X Histidine/Sucrose, mAbN at 0.8 mg/mL diluted in Bf1X Acetate/Sucrose, and ADC at 0.8

Table 1
Summary of model plastic surfaces and medical plastic surfaces used in this study, including the container category and type, supplier and reference, the corresponding name given in the present study, and the sterilization process (information given by the suppliers). Lot corresponds to the lot number of the bag.

Container Category	Container type	Supplier and Reference	Name	Sterilization Process
Model surfaces	Polystyrene96-well plate	Greinerbio-one −655101	PS plate	Nonsterile
	Polypropylene96-well plate	Greinerbio-one −650201	PP plate	Nonsterile
	Polyvinylchloride96-well plate	Corning −2595	PVC plate	Nonsterile
IV Empty Administration bag	PO empty bag Easyflex 250 mL	Macopharma (YZG0419EU) Lot: 20C251S	PP Bag-1	Gamma Radiation
IV Administration bags	PO bag Easyflex NaCl 0.9 % 250 mL	Carelides Macopharma (ACG0419FR) Lot: 22060036	PP Bag-1 NaCl	Autoclave after filling
	PO bag Freeflex NaCl 0.9 % 250 mL	Fresenius Kabi(2999511) Lot: 13QLF131	PP Bag-2 NaCl	Autoclave after filling
	PO bag freeflex G5% 250 mL	Fresenius Kabi(2998511) Lot: 13RLF171	PP Bag-2 G5%	Autoclave after filling
	PVC bag Perfudom® NaCl 0.9 % 250 mL	Bioluz (3400933308674) Lot: 220771	PVC Bag NaCl	Autoclave after filling
	PVC bag Perfudom® G5% 250 mL	Bioluz (3400933308094) Lot: 220259	PVC Bag G5%	Autoclave after filling
Manufacturing bag	NovaSeptum 50 mL	Millipore (1711-10050) Lot: 201112-551	LD-PE Bag	Beta irradiation at ≥25 kGy according to ISO 11137

mg/mL diluted in Bf1X Acetate/Sorbitol. The concentration of mAbs and ADC were chosen to represent the dilution of mAb concentration within the bags recommended for injection preparations. mAb and ADC adsorption was examined in the presence of surfactants, including PS80, PS20, or P188, across a concentration range from 0 to 8000 ppm. Although the concentration range of surfactants within the bags varies depending on the type of surfactant, typically spanning a range of 10 to 2000 ppm, the surfactant concentrations were tested up to 8000 ppm for research purposes. All experiments were done at room temperature (21 °C).

The samples were prepared in deep wells of 2 mL in the following order: starting with the Bf1X, then adding the surfactant, and finally the mAb or ADC. The 96-well plates (both on model and medical surfaces with ELIBAG) were filled with 100 µL mAb solution per well and shaken during 15 min at 900 rpm (Heidolph Titramax vibrating platform microplate shaker). Then, each plate was emptied and washed 4 times with 200 µL of surfactant (PS80, PS20 or P188 at 200 ppm in the corresponding Bf1X depending on the mAb or ADC). After that, the wells were filled with PtG-HRP at 250 µg/L containing 200 ppm of PS80, PS20 or P188 and shaken for 20 min at 900 rpm. Four new washing steps with surfactant at 200 ppm in Bf1X (200 µL) were performed. For the ELIBAG device, after emptying the wells, the frame was opened, and the bottom-less plate was replaced with a new bottom-less plate to prevent signal detection of mAb or ADC adsorbed on the PS walls of the plate. For model 96-well surfaces, mAb adsorption was detected on both bottom and walls of each well. The respective surface areas for model (0.95 cm^2) and medical (0.32 cm^2) surfaces were used for data analyses and comparison purposes. The surface area covered by the liquid meniscus movement during shaking was not considered.

Control replica (n = 4), consisting of incubating the material surface with the corresponding mAb buffer alone (no mAb, no surfactant), followed by washing steps with the buffer containing 200 ppm of the corresponding surfactant, have been systematically included in the adsorption experiments. The averaged absorbance values of these control replica were deduced from the averaged absorbance values obtained with mAbs and surfactants to account for potential non-specific PtG-HRP adsorption on the materials.

For the enzymatic reaction, 100 µL of 3,3′,5,5′-Tetramethylbenzidine (TMB) ready-to-use (Sigma reference T8665) was added in each well and shaken for 30 s at 900 rpm, followed by adding 50 µL of H_2SO_4 0.5 M (Acros organics reference 124640010) to stop the reaction. PtG-HRP bound to the adsorbed mAb was monitored by absorbance (λ = 450 nm) on a Tecan Infinite M1000 multimode microplate reader (TECAN USA, Boston, MA). Prior to the absorbance measurement, the contents of the wells were carefully transferred into a transparent polystyrene (PS) flat-bottom microplate (Greiner, 655101) for both model and medical surfaces. This ensured a standardized absorbance measurement for all the surfaces under investigation, thereby eliminating a bias due to well geometries. ELISA results represent mean values and their respective standard deviations obtained from a minimum of 3 independent experiments with 4 replicate wells per tested condition.

We have previously established a calibration method based on the enzyme activity of the secondary protein-HRP conjugate in solution [21]. This calibration method allows correlating the level of absorbance with the mass of secondary protein-HRP in solution. As previously described, for ELISA in plate, the surface area in contact with the solution considered was the bottom and the walls of the well with 100 µL per well, corresponding to 0.95 cm^2. For ELIBAG, the surface area in contact with the solution considered was only the bottom of the well (*i.e.*, the surface of the bag), 0.32 cm^2. Therefore, the results are presented in terms of adsorbed PtG-HRP per surface area, for mAbA, mAbN and ADC.

The schematic representation of the multiparameter (mAb-surfactant-surface) methodology employed to examine the compatibility between mAb formulations and materials is illustrated in Fig. 1. As previously described, medical bags were positioned within the ELIBAG device, enabling the analysis of diverse mAb-based formulations involving various combinations of mAbs and surfactants, within the 96 wells of the designed ELIBAG device. The adsorption of mAb directly on the medical surface was detected depending on the mAb modality, surfactant type and concentration, and material surface.

2.2. Surface characterization

2.2.1. Contact angle

The water contact angles (WCA) on the model surfaces and IV and manufacturing bags were measured with a drop shape analyser (DSA100 Krüss Scientific). A drop of 1 µL of miliQ water was deposited on the surface of the material and the WCA was measured. WCA values were obtained from a minimum of three separate drops deposited on different areas on each sample. To achieve a flat surface for the plastic bags, suitable for WCA measurement, a 1 cm^2 piece was fixed with a double-sided adhesive on a glass slide. The internal surface of the bags was analysed. To analyse the WCA within the wells of the 96-well plates, the well bottoms or walls were previously cut to measure the hydrophobicity of the internal surface of the wells.

2.2.2. Attenuated total reflectance-fourier transform infrared spectroscopy

GATR (grazing angle attenuated total reflectance)-FTIR was performed using a VariGATR™ accessory (Harrick Scientific), a single reflection ATR accessory with a Germanium crystal plate, installed in a Bruker Vertex 70v. Samples were cut at a specific size and pressed against the Ge crystal to ensure effective optical coupling. Spectra were collected in a wavenumber range between 400 and 4000 cm^{-1} and under a dry nitrogen purge with a 4 cm^{-1} resolution (256 scans). A

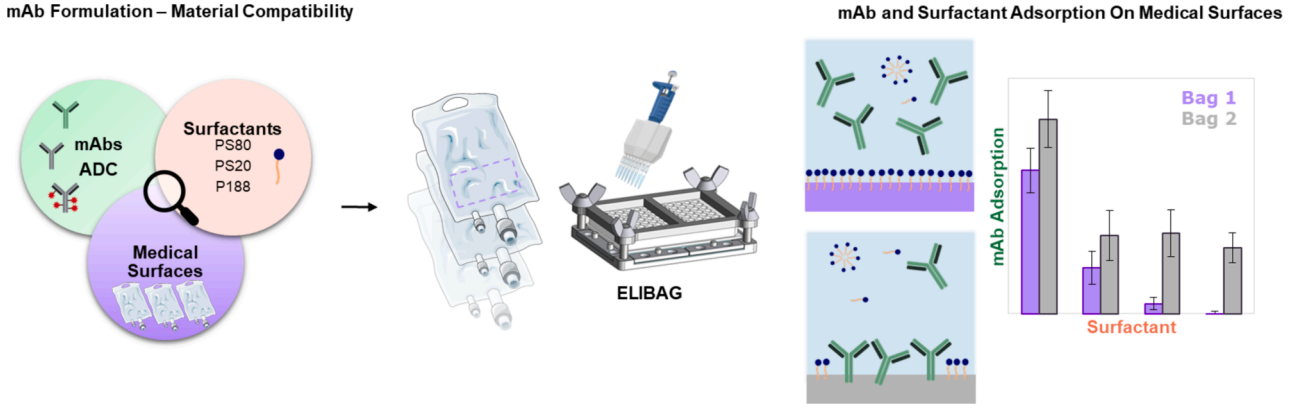

Fig. 1. Schematic representation of the methodology used to investigate the adsorption of mAbs and surfactants directly on medical surfaces. Medical bags were positioned in the ELIBAG device, facilitating the analysis of a diverse array of mAb-based formulations comprising various combinations of mAbs and surfactants.

GloBar MIR source and a broadband KBr beam splitter were employed. Background measurements were obtained from the bare Ge crystal under vacuum. All spectra were collected at room temperature.

Sample preparation was performed by cutting the samples to a specific size of 1.5 cm^2 approximately for the analysis of the internal surface of model and medical surfaces (in contact with the formulation).

The software used for data analysis was OPUS version 8.5.29 (Bruker). The databases employed for surface composition identification included Polymer.S01 from the Bruker OPUS Library and ATR-LIB COMPLETE-3-472-2. S01. However, it is important to note that these databases do not include all additives and surface compositions related with these materials.

2.2.3. X-ray Photoelectron Spectroscopy

X-Ray Photoelectron spectra were recorded on a ThermoScientific K-Alpha spectrometer using a monochromatized Al Kα radiation source (1486.6 eV), in ultrahigh vacuum (10^{-8} mbar) at room temperature. The X-Ray beam area (spot size) was adjusted to 400 μm in diameter. Analyses were conducted at 90° angles between the sample surface and the analyzer. The photoelectrons emitted were inspected with a 180° double focusing hemispherical analyzer and a 128-channel detector. The binding energy (BE) scale of the spectrometer is regularly calibrated by the positions of the peaks of Au 4f7/2 (83.9 ± 0.1 eV) and Cu 2p3/2 (932.8 eV ± 0.1 eV) core levels of pure gold and copper metals. The spectra were acquired in the constant analyzer energy mode using a pass energy of 30 eV and a step size of 0.1 eV for core levels, and a 100-eV pass energy has been used for the general survey spectrum (step 0.5 eV).

Sample preparation was performed by cutting the samples at a specific size of 1 cm^2 approximately for the analysis of the internal surface of model and medical surfaces. For the case of model surfaces (multiwell plates), the internal surface of the well was analysed. The analysed surface area per sample was 400 μm^2 with a penetration depth of 5–10 nm.

The spectra shown have been averaged over 3 scans for the survey and 10 scans for the core levels. The flood gun was used to neutralize charge effects on the surface. Peak analysis and decompositions were performed using Thermo Scientific Advantage software. Core peaks were analyzed using a non-linear Shirley-type background and quantification was performed based on Scofield's relative sensitive factors.

3. Results and discussion

Previous investigations have shown that the protection efficacy of surfactants at the solid/liquid interface depends on the mAb modality, surfactant, and type of model surface [8,16]. In this study, by using the previously developed ELIBAG device [21], we have investigated the protection efficacy of a variety of mAbs and surfactants directly on medical surfaces for the first time in real use conditions (*ie.* at the medical surface/formulation interface).

For the study, we examined the adsorption of two monoclonal antibodies, named mAbA and mAbN, and one antibody-drug conjugate, ADC, which is mAbN conjugated to a cytotoxic drug. The three commonly used surfactants in parenteral formulations in the pharmaceutical industry, PS80, PS20 and P188, were investigated. The adsorption of mAbs and ADC was detected and quantified by a secondary protein, PtG-HRP, which binds specifically to the mAb, and results are expressed as the mass of adsorbed PtG-HRP per surface area. A calibration based on HRP activity in solution was used. A variety of medical surfaces, including PP, PVC, and LD-PE bags, and model surfaces, typically 96 well-plates made of PS, PP and PVC, were evaluated.

Our multiparameter approach has led us to compare representative mAb-based formulations across a variety of plastic surfaces. In this section, we highlight key observations and provide insights into factors that can affect mAb adsorption directly on medical surfaces. These investigations hold the potential to benefit material compatibility studies during drug product development, particularly in in-use studies. We first compared the adsorption of mAbA, mAbN and ADC in the absence of surfactants, directly on medical and model surfaces. Then, we compared the protection efficacy of the three surfactants to prevent mAbA, mAbN and ADC adsorption on model and medical surfaces. In addition, we have also investigated the material surface characteristics in order to explore potential correlations between material surface composition and mAb and surfactant adsorption profiles at the solid/liquid interface.

3.1. Adsorption of mAbA, mAbN and ADC on plastic surfaces

The detection of mAbA, mAbN, and ADC in the absence of surfactant was achieved using PtG-HRP, both on medical surfaces (Fig. 2) and multiwell plates (supplementary Fig. S1). In the absence of surfactants, all mAb modalities adsorb on all the tested surfaces in a mass range comprised between 4.6 ± 0.9 ng/cm^2 and 12.8 ± 1.4 ng/cm^2 of adsorbed PtG-HRP. Remarkably, the levels of adsorbed PtG-HRP for mAbA and ADC were either similar or higher than those for mAbN for any given surface (Fig. 2). For example, when considering PVC Bag NaCl, the highest quantity of adsorbed PtG-HRP was recorded for mAbA (12.8 ± 1.4 ng/cm^2), followed by ADC (6.3 ± 1.4 ng/cm^2), and mAbN (4.6 ± 0.9 ng/cm^2). These differences in adsorbed PtG-HRP levels contigent upon the mAb modality varied depending on the material surface, with a consistent trend of elevated adsorption levels for mAbA and ADC compared to mAbN. Equivalent results were obtained on PS, PP and PVC plates, in which the levels of adsorbed PtG-HRP for mAbA and ADC were also similar or higher than for mAbN (supplementary Fig. S1).

The amount of protein adsorbed on a surface is the result of a combination of several phenomena, including the concentration of protein at the interface, the strength of protein-surface and protein–protein interactions and the footprint of the adsorbed molecule, resulting in a packing density with a given molecular orientation of the adsorbed species. These phenomena are dependent on the intrinsic properties of each protein [23]. Previous investigations revealed that the adsorption profiles at the air/liquid interface were different for three mAb modalities, a mAb, an ADC, and a BsAb (bispecific mAb). Notably, the bsAb exhibited a higher surface sensitivity compared to the mAb and the ADC [8]. Furthermore, Džupponová V. *et al.* [24] recently investigated the adsorption of two mAbs at the solid/liquid interface using model PS microparticles. Their findings revealed that despite the fact that both mAbs are the same isotype and subclass (IgG1), the adsorption depends on several sequence-related factors. An interesting recent study using MD simulations [25] pinpoints the effect of certain amino acids on the surface activity of a mAb and the authors conclude that minor structural modifications can significantly affect the interface adsorption potential. Hence, our observed differences in the adsorption behaviour of mAbA, mAbN and ADC on PP, PVC, and LD-PE bags, as well as on PS, PP and PVC plates, could, at least in part, be attributed to the intrinsic properties of each protein. Moreover, the comparative analysis between mAbN and ADC (mAbN conjugated with a cytotoxic drug), revealed a higher amount of adsorbed ADC on the hydrophobic plastic surfaces. This could be related to a higher overall hydrophobicity of the ADC, in comparison with mAbN, conferred by the chemical nature of the linked drug molecule. The hydrophobicity of the drug could increase the affinity of ADC for plastic surfaces [14], hence the increased adsorption on the tested hydrophobic materials.

3.2. Surfactant protection efficacy depends on the mAb modality on a given surface

Based on our own and other previous investigations, surfactant protection efficacy to prevent mAb adsorption depends on the surface, for a variety of commercially available multiwell plates made of PS, PP, PVC, COC and PC [16] and other model surfaces [17]. The aim of the present study was to assess surfactant protection efficiency directly on medical plastic surfaces for the first time, exploring the potential correlations with surface characteristics. Therefore, we investigated the

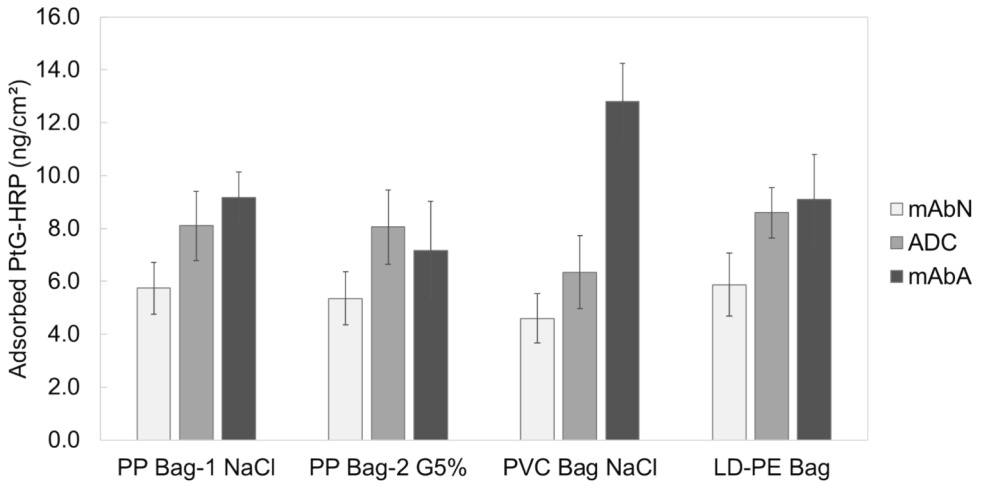

Fig. 2. Adsorbed PtG-HRP depending on the mAb modality and surface for PP Bag-1 NaCl, PP Bag-2 G5%, PVC Bag NaCl, and LD-PE Bag. mAbA was incubated at 2 mg/mL, and mAbN and ADC at 0.8 mg/mL in their corresponding Bf1X, as indicated in Materials and Methods. The adsorbed PtG-HRP values are normalized to the absorbance measured for Bf1X without mAb. Error bars represent standard deviations (n = 12).

surfactant protection efficacy of PS20, PS80 and P188, to prevent mAbA, mAbN and ADC adsorption on a variety of medical and model surfaces. The protection efficacy of the 3 surfactants and 3 mAb modalities on all the tested surfaces (plates and bags) are summarised in supplementary Fig. S2 and Fig. S3. In the following sections, we have highlighted key observations obtained from the results across the variety of surfaces, surfactants and mAb modalities.

In general, we found that the protection efficacy of surfactants depends on the mAb modality and material surface for the tested conditions. To illustrate this point, Fig. 3, presents the results obtained for PP Bag-1 NaCl, comparing the adsorption of mAbA (Fig. 3A), mAbN (Fig. 3B), and ADC (Fig. 3C) depending on the surfactant concentration and type. Interestingly, PS20 at 50 ppm presented a better protection efficacy than PS80 and P188 in preventing mAbA adsorption on PP Bag-1 NaCl (Fig. 3A). This behaviour was also true for mAbN (Fig. 3B). In addition, we have also monitored that PS20 protection efficacy at 50 ppm was remarkably better than PS80 and P188 on LD-PE Bag for mAbA, and on PS and PP plates for the 3 mAb modalities (supplementary Fig. S3A and Fig. S2AB, respectively).

Concerning ADC adsorption on the PP bag-1 NaCl (Fig. 3 C), all three surfactants presented comparably low protection efficacy in the concentration range up to 1000 ppm, especially P188, which, even at higher concentrations, demonstrated less protection than polysorbates. P188 appeared to be less efficient than PS80 and PS20 for preventing mAbN and ADC adsorption on PP Bag-1 NaCl, contrasting with the protective effect observed for mAbA. For ADC, PS80 seems to be the most efficient surfactant, albeit only at high concentrations (1000 and 8000 ppm, Fig. 3C). P188 has a higher hydrophilic-hydrophobic-balance (HLB) value (29) compared to PS80 (15) and PS20 (16.7) [22]. Thus, the findings showing a lower protection efficacy of P188 on some surfaces and for some mAbs (as in Fig. 3B and Fig. 3C for example) may be explained by a lower affinity of P188 for hydrophobic surfaces and/or a less effective kinetic competition with the mAb for adsorption under the tested conditions.

Overall, our observations indicate that the protection efficacy of both polysorbates, PS20 and PS80, demonstrated a better or equivalent protective efficacy compared to P188, both on bags and plates. This tendency aligns with a recent study by Zürcher et al. [17], in which they showed that PS20 and PS80 presented a better protection efficacy than P188 to prevent mAb adsorption (at 1 mg/mL) on a model hydrophobic interface (*cyclo*-olefin-copolymer, COC, nanoparticles). Furthermore, Doshi et al. [26] showed that PS20 was more effective in preventing mAb particle formation (1 mg/mL) than PS80 under agitation stress in glass vials. They demonstrated that PS20 at 50 ppm reduced mAb soluble aggregates, in comparison to PS80, for which more than 100 ppm was needed to decrease mAb soluble aggregates. Additionally, Vaclaw et al. [27] compared protein particle formation formulated with PS80 or PS20 (at 10 and 100 ppm) at the air/liquid interface. They show that PS20 is more effective than PS80 at mitigating the formation of larger particles in the bulk solution for 2 mAbs (at 0.5 mg/mL). Additionally, a recent study by Escobar et al. [13] revealed that PS20 (at 25 ppm and 200 ppm), mitigated subvisible particle formation of mAb at 10 mg/mL,

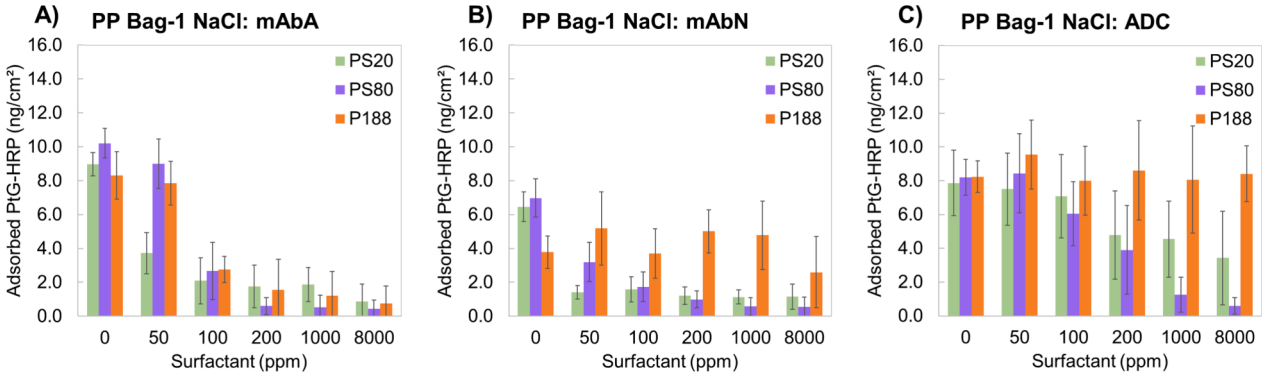

Fig. 3. Surfactant protection efficacy to prevent A) mAbA (2 mg/mL), B) mAbN (0.8 mg/mL) and C) ADC (0.8 mg/mL) adsorption on PP Bag-1 NaCl. Adsorbed PtG-HRP values are normalized to the absorbance measured for Bf1X without mAb. Error bars represent standard deviations (n = 12).

and that the air/liquid interface was surfactant-dominated. Hence, even at concentrations lower than its CMC value (72 ppm for PS20[22], PS20 exhibited greater efficacy compared to PS80 at the air/liquid interface and in preventing mAb particle formation. While these studies do not directly address the medical bag/formulation interface, they show valuable insights into the superior efficiency of PS20 compared to PS80, which aligns with our observations of enhanced PS20 protection efficacy at 50 ppm on certain medical and model surfaces. When comparing chemically PS80 and PS20, both polysorbates present a hydrophilic polyoxyethylene sorbitan head group; however, the hydrophobic tail of fatty acid ester is oleic acid (unsaturated chain structure) for PS80, and lauric acid (linear chain structure) for PS20 [28]. Surfactants with linear chains tend to pack more tightly, potentially leading to more compact adsorption on hydrophobic surfaces compared to those with unsaturated chains [29]. Consequently, we could hypothesize that in the competition between surfactants and mAbs at interfaces, PS20 could provide better protection efficacy to prevent mAb adsorption than PS80 (at 50 ppm), due to a more compact packing at the hydrophobic surface. At higher surfactant concentrations (over 100 ppm), both polysorbates present in general similar effectiveness.

From a formulation point of view, PS80 and PS20 are employed in concentration ranges of 1–4000 ppm and 40–5000 ppm, respectively, while P188 is used at concentrations between 200 and 8000 ppm. Therefore, most mAb formulations contain surfactants at concentrations higher than their critical micelle concentration (CMC) [30]. Since drug products are typically diluted at least 2-fold in IV bags prior to administration [31], the surfactant protection efficacy to prevent mAb adsorption might be affected by the decreased surfactant amount in the bags. For example, PS80 is much less efficient at protecting mAbA in the PP bag-1 NaCl (Fig. 2 A) for concentrations below 200 ppm than at this concentration or above. We thus confirm that the protection efficacy of surfactants directly on medical bags does not only depend on the surfactant type and concentration but also on the material in contact with the formulation.

3.3. Surfactant protection efficacy depends on the material for a given mAb modality

Depending on the bag's material, we have shown that the addition of surfactant to the formulation can effectively protect certain mAb modalities from adsorption on the plastic surface. The protection efficacy of PS80 to prevent mAbA, mAbN and ADC is presented for different medical bag materials, made of PP, PVC, and LD-PE (Fig. 4). For mAbA, PS80 protection was more effective on PP Bag-1 NaCl and LD-PE Bag in comparison with PP Bag-2 G5% and PVC Bag NaCl (Fig. 4A). For mAbN, PS80 was effectively preventing mAbN adsorption across the four tested bags (Fig. 4B). In the case of ADC, PS80 appeared to have a better protection efficacy on PP Bag-1 NaCl, PVC bag NaCl and LD-PE Bag in comparison with PP Bag-2 G5% (Fig. 4C).

Additional data obtained for the other surfactants (PS20 and P188) and for PS80 on model plates and medical surfaces are presented in supplementary Fig. S4 and Fig. S5, respectively. Interestingly, for the PP bags, either there was an excellent protection efficacy of the polysorbates to prevent the adsorption of the three mAb modalities (typically in PP Bag-1 NaCl) or the protection was inefficient (PP Bag-2 G5%) (Fig. 4A–C). For P188 on PP bags, it exhibits a comparable behaviour to polysorbates regarding mAbA (Fig. S5D). There is a trend indicating better P188 protection efficacy to prevent mAbN adsorption on PP Bag-2 G5% compared to PP Bag-1 NaCl (Fig. S5E). However, despite its effectiveness on some surfaces, P188 did not prevent ADC adsorption on both types of PP bags, even at concentrations higher than 1000 ppm (Fig. S5F).

On PVC surfaces, the surfactant protection efficacy was in general worse than on other materials (Fig. S2 and Fig. S3), especially for mAbA and ADC on PVC Bag and PVC Plate. For mAbN however, polysorbates presented an intermediate protection efficacy on PVC surfaces (Fig. 4B and supplementary Fig. S4B and E and Fig. S5B and E). Interestingly, on the LD-PE Bag the protection efficiency for every mAb modality and surfactant tested was effective, albeit in slightly different concentration ranges.

Previous in-use studies have investigated mAb-container compatibilities across various medical bags, principally made of PVC, PO, and PE [19,20,32]. Generally, they examined mAb stability in solution by measuring mAb aggregates, subvisible particles and other parameters such as particle size and morphology, according to best practices [18]. Because multiple interfaces are simultaneously present when a formulation is agitated in a container (solid–liquid, liquid–air and the dynamic triple line), one should be careful when comparing individual interfacial contributions. Kumru et al. demonstrated that mAb (1 mg/mL) losses in PVC bags were higher (25 %) than in PO bags (8 %), in the absence of PS20 during IV agitation studies after 6 h incubation, detected by SE-HPLC [20]. In the presence of PS20 at 150 ppm, mAb losses were lower than 1 % for both types of bags, highlighting the importance of adding surfactants to the formulation. Our results align with Kumru OS *et al.* for the case of mAbN, in which PS20 at 100 ppm prevented mAbN adsorption on all the bags (PP, PVC and LD-PE) (Fig. S5B). However, this was not the case for the other mAb modalities, mAbA and ADC, in which the addition of PS20 did not prevent mAbA and ADC adsorption on PVC bags and PP Bag-2 G5% (Fig. S5A and C, respectively). This might be due to the fact that we investigate adsorption at the solid–liquid interface, which is only one of the interfacial contributions in agitated containers.

Also in PO and PVC bags, Sreedhara et al. [19] performed in-use studies on three different mAbs (between 1 and 5 mg/mL) with PS20 (between 3 and 40 ppm) under agitation conditions for 24 h. They

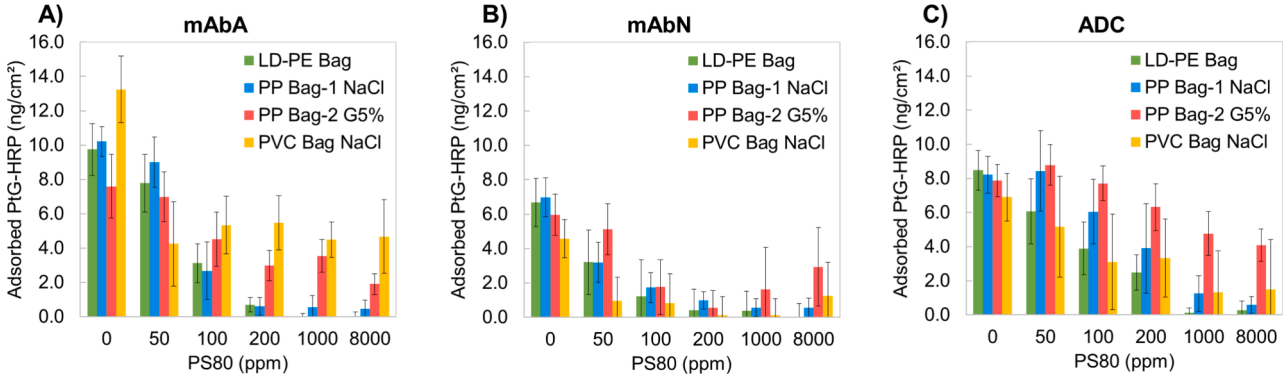

Fig. 4. PS80 protection efficacy to prevent mAbA (2 mg/mL) (A), mAbN (0.8 mg/mL) (B) and ADC (0.8 mg/mL) (C) adsorption on LD-PE Bag, PP Bag NaCl, PP Bag G5% and PVC Bag NaCl. Adsorbed PtG-HRP values are normalized to the absorbance measured for Bf1X without mAb. Error bars represent standard deviations (n = 12).

reported that many of the tested mAbs should not be diluted and stored in IV bags over extended periods of time, showing that the sensitivity of mAb aggregation depends on the mAb. In addition, Kim et al. [32] evaluated the stability of Rituximab (Truxima®) on PE and PVC bags. They demonstrated that the mAb (at 10 mg/mL) with 700 ppm of PS80 was stable after 6 weeks at 2–8 °C + 1 day at 25 ± 2 °C. Hence, numerous mAb stability studies have investigated mAb-container compatibilities with a variety of containers, formulations and agitation conditions, showing that mAbs may behave differently in different brand products [33]. Even if the formation of protein aggregates in aqueous solution is frequently initiated by interactions between protein and interfaces [6], the majority of studies have focused on mAb stability in solution rather than directly measuring mAb adsorption on medical surfaces, highlighting the need of mAb adsorption measurements directly at the medical bag/formulation interface.

3.4. Model surfaces do not fully represent medical surfaces for mAb and surfactant adsorption

Our study includes investigations on commercially available plastic model surfaces in order to investigate if these accurately replicate the adsorption behaviour of mAbs and surfactants observed in medical surfaces made from the same plastic polymer. As previously presented in Table 1, there are PP model and medical surfaces, as well as PVC model and medical surfaces. However, there is no LD-PE model surface available in the 96-well format, to use as a comparison with the LD-PE manufacturing bag. Therefore, in this section, we compare the protective effect of PS20, PS80 and P188 to prevent mAbA adsorption on PP and PVC model and medical surfaces.

For PP surfaces, all surfactants were effective in preventing mAbA adsorption on the PP plate (this holds also true for the other mAb modalities, Fig. S2B, E and H), while an intermediate protection efficacy was observed on PP Bag-2 G5% (Fig. 5A–C). In the case of PVC surfaces, surfactants were not able to prevent mAbA adsorption efficiently, even at 8000 ppm (illustrated in Fig. 5D–F), and an intermediate protection efficacy was detected for the PVC Bag NaCl. Hence, the PVC model surface represents a more comparable adsorption behaviour to the analysed PVC IV Bag, while the PP model surface can represent the adsorption behaviour of some medical PP surfaces (like PP Bag-1 NaCl, supplementary Fig. S3), but it does not fully represent all the tested PP bag surfaces (like PP Bag-2 G5%). Similar observations were made for mAbN and ADC, for which adsorption on model surfaces do not fully behave as on plastic medical surfaces made from the same polymer (supplementary Fig. S2 and Fig. S3).

Thus, even when model surfaces and medical surfaces share the same primary polymer composition, such as PP or PVC, differences in the manufacturing, presence of additives and/or sterilization methods could significantly influence plastic surface characteristics, and thus impact surfactants' protection efficacy to prevent mAb adsorption. Hence, it highlights the necessity of measuring mAb adsorption directly on medical bags to ascertain formulation efficacy and mAb stability.

3.5. Material surface composition impact on surfactant protection efficacy to prevent mAb adsorption

We aimed to investigate the protection efficacy of different surfactants on surfaces made of the same primary polymer: polypropylene. For that, we have investigated PS80, PS20 and P188 protection efficacy for mAbA adsorption on four PP Bags: PP Bag-1, PP Bag-1 NaCl, PP Bag-2 NaCl and PP Bag-2 G5%. PP Bag-1 and PP Bag-1 NaCl are from the same supplier, and PP Bag-2 NaCl and PP Bag-2 G5% are also from the same supplier, different than the previous supplier (details in Table 1).

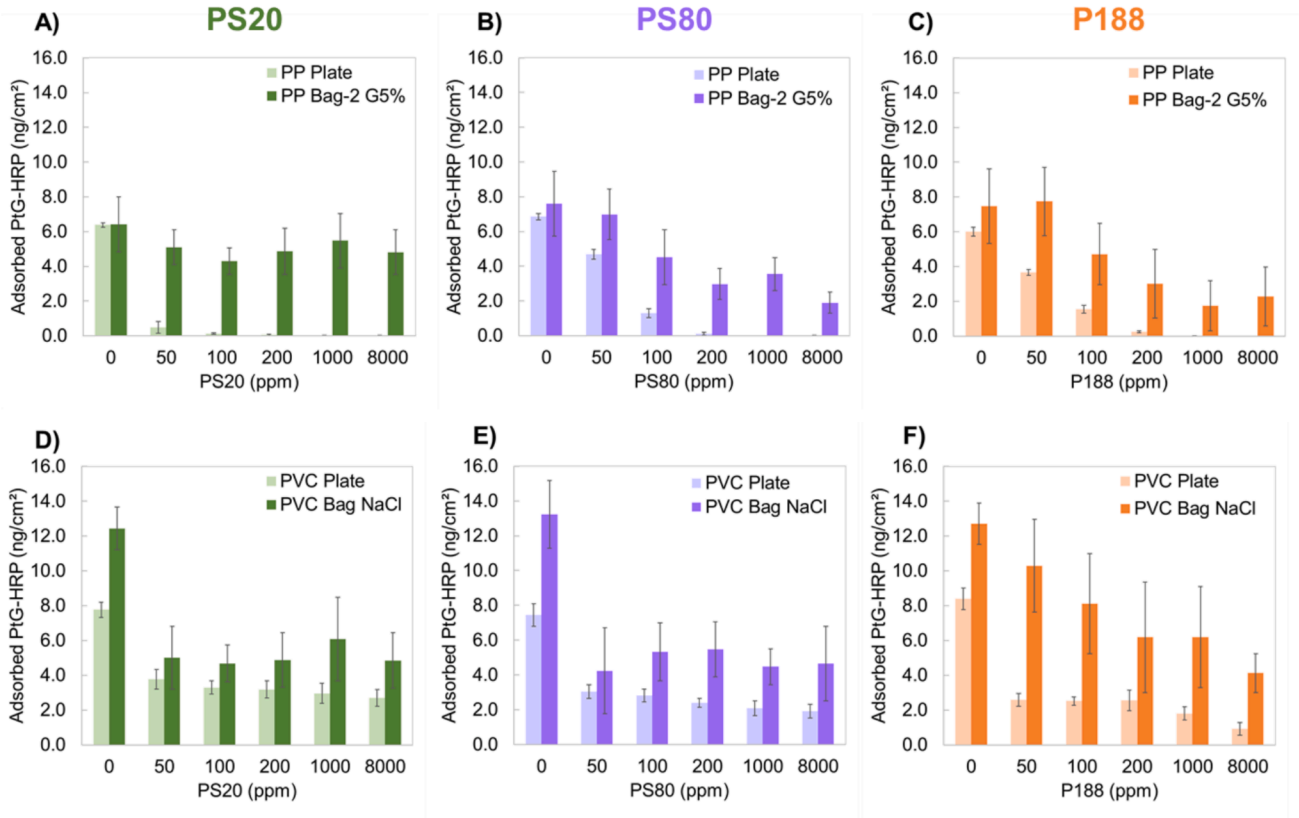

Fig. 5. Surfactant protection efficacy of PS20 (A, D), PS80 (B, E) and P188 (C, F) to prevent mAbA (2 mg/mL) adsorption on PP plate (model surface) and PP bag-2 G5% (medical surface) (A-C) and on PVC plate (model surface) and PVC Bag NaCl (medical surface) (D-F). Adsorbed PtG-HRP values are normalized to the absorbance measured for Bf1X without mAbA. Error bars represent standard deviations (n = 12).

We demonstrate that bags made of the same primary polymer (PP) do not show the same adsorption profiles for mAbA and surfactants (Fig. 6). Interestingly, for PP Bag-1, PS20 presented a better protection efficacy at 50 ppm than for the other bags and surfactants at this concentration (Fig. 6A). This greater efficiency of PS20 was previously discussed in 3.2. Consistently the worst protection efficacy was measured for PP Bag-2 G5% with the three surfactants. PS80 prevented mAbA adsorption fully at concentrations higher than 200 ppm on PP Bag-1 and PP Bag-1 NaCl. However, on PP Bag-2 NaCl and PP Bag-2 G5%, PS80 concentrations as high as 8000 ppm were not able to fully prevent mAbA adsorption. For the case of P188, the adsorption profiles are similar for the four PP bags, with again, a tendency of a lower protection efficacy on PP Bag-2 G5%. In order to investigate the differences between mAb and surfactant adsorption profiles observed for the different PP bags, and identify potential correlations between material properties and adsorption profiles, we analysed the surface composition of both model surfaces and medical bags (Section 3.5.1 and Fig. 7).

3.5.1. *Surface characterization of model surfaces and medical bags*

The surface characteristics of both model and medical plastic containers used in this study are summarised in Table 2. A total of three plastic model surfaces and seven medical plastic bags were investigated. For each material, the internal surface was analysed by ATR-FTIR and WCA, as previously described (see Section 2).

For model surfaces, PS, PP and PVC were identified as the main components of the internal surface of the wells. For medical surfaces, the three main polymers were identified: PP for IV Bags, PVC with DEHP for IV bags, and LD-PE for the manufacturing pharmaceutical bag. DEHP is known as a common plasticizer additive in PVC bags [34]. Interestingly, it has been previously reported that DEHP droplets from PVC bags can cause protein aggregation and particle formation [35].

The surface hydrophobicity was measured by water contact angle on a piece of each surface. In terms of hydrophobicity, the tested surfaces ranged from less hydrophobic to more hydrophobic as follows: PS Plate < PVC Plate < PP Plate < LD-PE Manufacturing Bag < PP Bag-2 NaCl < PVC Bag NaCl < PVC Bag G5% < PP Bag-1 NaCl < PP Bag-2 G5% Bag < PP Bag-1. Overall, all the surfaces were in a range of hydrophobicity within 76.0° ± 4.7° and 96.0° ± 1.4°, as measured by WCA.

Regarding the sterilization process, model surfaces are non-sterile while medical surfaces are sterilized by different processes: PP Bag-1 is sterilized by gamma radiation, LD-PE Bag by beta irradiation, and the other bags by autoclaving after filling. This highlights the diversity of sterilization methodologies employed in the medical device industry to ensure rigorous sterile conditions.

No significant direct correlation between chemical composition and hydrophobicity of the material surfaces, or the sterilization process and the measured adsorption profiles, could be identified.

Finally, the surface composition was further investigated by XPS. Interestingly, we have detected the presence of silicon on some surfaces, with the highest content of silicon on PP Bag-2 G5% (6.91 Si/C ratio), followed by PP Bag-2 NaCl (3.66), PVC Bag NaCl (3.64), PVC Bag G5% (2.06), PS Plate (1.66), PVC Plate (1.02), PP Plate (0.89) and PP Bag-1 NaCl (0.6). There was no silicon detected on PP Bag-1 and LD-PE Bag (below detection limit). The XPS analysis of model and medical surfaces including surface composition of major elements in atomic% and ratio O/C, Si/C, Ca/C and Cl/C is included in Supplementary Table S1.

We found that for PP Bag-2 G5%, which presented the highest silicon content on the surface, the protection efficacy of the three surfactants was less efficient than in the presence of a lower or undetectable amount of silicon on other PP bags. We compared the protection efficacy of PS20, PS80 and P188 at different concentrations (from 50 to 8000 ppm) to prevent mAbA adsorption, with the silicon content of PP bags (Si/C ratio), illustrated in Fig. 7. We observed that the protection efficacy of the three surfactants is decreased with an increase of the silicon content present on the surface of the PP bags. The correlation between protection efficacy and Si content is statistically significant for all the surfactants tested (supplementary Fig. S9 and Table S2).

Notably, PS20 protection efficacy is reduced from 95 % to 20 % for all the surfactant concentrations tested with increasing presence of Si (Fig. 7A). In the case of PS80 (Fig. 7B) and P188 (Fig. 7C), at 50 ppm, the surfactant protection efficacy is always lower than 20 % for PS80, and 10 % for P188, independently of the silicon content. However, as the concentration of surfactant increases from 100 to 8000 ppm, there is a noticeable decrease in the protection efficacy depending on the silicon content. This protection efficacy was reduced from 95–100 % to 60–80 % for PS80 and P188 (200–8000 ppm). At 100 ppm, the efficiencies of PS80 and P188 were reduced by 40 % and by 20 %, respectively, for the highest Si content. While PS20 demonstrated superior efficiency in preventing mAbA adsorption at 50 ppm (on PP Bag-1, without silicon detected on the surface), it also exhibited the highest impact when silicon was detected on the surface, with a decrease in protection efficacy over 50 %. Additionally, we have detected the presence of silicone oil particles by Micro-Flow Imaging (MFI) in solutions incubated in PP Bag-2 G5%, and in PP Bag-1 NaCl (data not shown). Moreover, the presence of silicon on the internal surface of medical bags was corroborated through Laser-Induced Breakdown Spectroscopy (LIBS) analysis (data not shown). Notably, LIBS offers a superior penetration depth of 5 μm in comparison with XPS, which typically operates within the range of 5–10 nm. Thus, the elemental analysis provided by LIBS corresponds to a deeper layer of the material.

The presence of silicon on medical containers was previously reported on closed system transfer devices (CSTD) by Wozniewski et al.

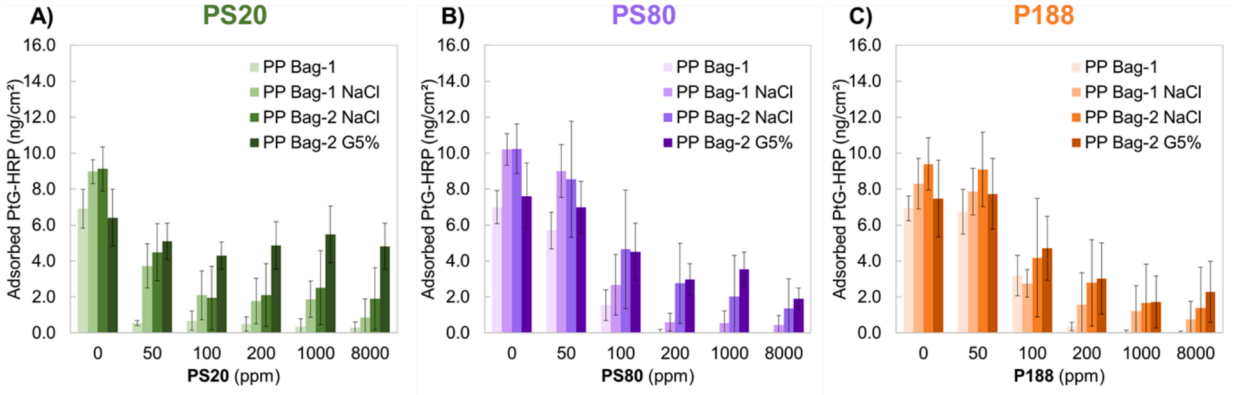

Fig. 6. Surfactant protection efficacy of PS20 (A), PS80 (B) and P188 (C) to prevent mAbA (2 mg/mL) adsorption on PP bags (PP Bag-1, PP Bag-1 NaCl, PP Bag-2 NaCl, and PP Bag-2 G5%). Adsorbed PtG-HRP values are normalized to the absorbance measured for Bf1X without mAbA. Error bars represent standard deviations (n = 12).

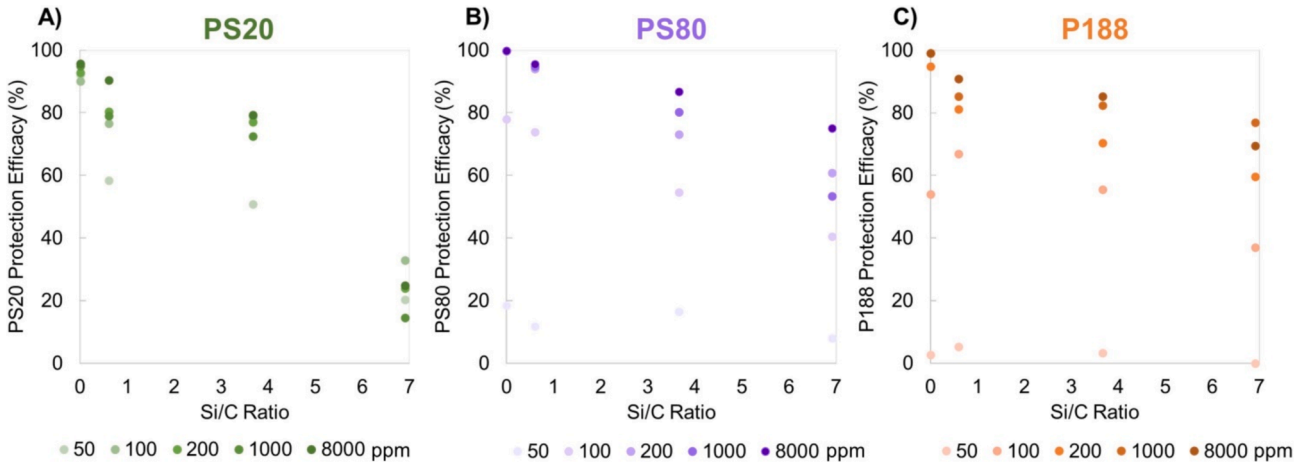

Fig. 7. Surfactant protection efficacy of PS20 (A), PS80 (B) and P188 (C) to prevent mAbA (2 mg/mL) adsorption depending on the silicon content (Si/C ratio detected by XPS) of PP bags (PP Bag-1, PP Bag-1 NaCl, PP Bag-2 NaCl, and PP Bag-2 G5%). The protection efficacy is represented as a function of surfactant concentration in the range from 50 ppm to 8000 ppm (light to dark colours). The percentage of surfactant protection efficacy is calculated relative to the condition of mAb adsorbed without surfactant. 0 % corresponds to a bad surfactant protection efficacy; 100 % corresponds to a total surfactant protection efficacy. Si/C ratio calculated as (atomic% Si divided by atomic% C) × 100.

Table 2
Surface characterization of containers. Contact layer composition was obtained by ATR-FTIR; hydrophobicity by WCA; and Si/C ratio detected by XPS and calculated as (atomic% Si divided by atomic% C) × 100. PS, polystyrene; PP, polypropylene; PVC, Polyvinylchloride; DEHP: di(2-ethylhexyl) phthalate; LD-PE, low-density polyethylene. ND: Non-detectable.

Container Category	Name	Contact Layer Composition	Water Contact Angle (°)	Si/C ratio
Model surfaces	PS Plate	Polystyrene	76.0 ± 4.7	1.66
	PP Plate	Polypropylene	84.7 ± 2.5	0.89
	PVC Plate	Polyvinylchloride	80.1 ± 2.0	1.02
IV Empty Administration bag	PP Bag-1	Polypropylene	96.0 ± 1.4	ND
IV Administration bags	PP Bag-1 NaCl	Polypropylene	94.9 ± 4.4	0.6
	PP Bag-2 NaCl	Polypropylene	87.6 ± 1.3	3.66
	PP Bag-2 G5%	Polypropylene	95.3 ± 2.8	6.91
	PVC Bag NaCl	Polyvinylchloride + DEHP	91.1 ± 2.0	3.64
	PVC Bag G5%	Polyvinylchloride + DEHP	91.1 ± 3.4	2.06
Manufacturing bag	LD-PE Bag	Low-Density Polyethylene	86.5 ± 2.2	ND

[36]. They detected significant amounts of silicone oil, found as sub-visible particles, in most of the CSTDs that they tested. Silicon was also detected on the surface of PVC tubing with a content of 0.2 atomic%, detected by XPS [37]. For medical bags, such as IV bags and manufacturing bags, the silicon present on the surface might originate from an additive in the manufacturing or from a contamination. Potentially, silicone oil, known to be present on the tubing of prefilled bags, could have migrated from the tubing via the fill solution (NaCl, glucose) into the bag, where it is deposited on the inner surface. However, the origin of the silicon content is unknown, and further investigations would be necessary to clarify this point.

4. Conclusion

Our study marks the first attempt to evaluate mAb and surfactant adsorption directly on medical surfaces, specifically at the medical bag/formulation interface. We tested three different biotherapeutic antibodies: monoclonal antibody A (mAbA), monoclonal antibody N (mAbN), and an antibody-drug conjugate (ADC), based on mAbN linked to a cytotoxic drug. We explored the role of three non-ionic surfactants, polysorbate 80 (PS80), polysorbate 20 (PS20) and poloxamer 188 (P188), in mitigating mAb-surface interactions, particularly focusing on their efficacy in preventing mAb adsorption. We evaluated the adsorption of mAbs and surfactants on a variety of plastic medical surfaces (IV administration bags and manufacturing bags), and hydrophobic model surfaces (in the format of 96-well plates). The main surface composition of the tested plastic surfaces is polypropylene (PP), polyvinyl chloride (PVC) and low-density polyethylene (LD-PE).

Our findings demonstrated that the protection efficacy of surfactants depends on the mAb modality, surfactant type and concentration, and surface material. In the absence of surfactant, mAbA and ADC tend to adsorb more than mAbN on both medical and model surfaces, which illustrates the impact of inherent molecular characteristics of the biomolecule. Moreover, the addition of a hydrophobic drug on mAbN, resulting in the ADC molecule, induces a higher affinity for its adsorption on hydrophobic surfaces compared to mAbN. When surfactants were added in the formulation, polysorbates generally exhibited a better or equivalent protection efficacy in preventing mAb adsorption, compared to P188.

Regarding the material surface impact, the surfactant protection efficacy on PVC surfaces was generally inferior compared to other materials, especially for mAbA and ADC. In contrast, surfactants were effective on LD-PE bags for all the tested mAb modalities and surfactants. Additionally, our study revealed that bags made of the same primary polymer (PP) exhibited different adsorption profiles. This observation led us to investigate material surface characteristics, exploring potential correlations of the protective efficacy of surfactants with the medical surface composition. We highlight that the presence of silicon on the surface of the polymeric bags can impact molecular adsorption profiles. Medical surfaces, such as those from IV and manufacturing bags, present complex characteristics including a variety of materials, presence of additives, various sterilization processes, and they can even be made of multilayer systems of different polymers. Thus, it is important to measure mAb and surfactant adsorption directly on

these medical surfaces. Further investigations regarding the impact of surface additives and/or leachable are required to gain a deeper understanding of protein adsorption and the protective role of surfactants directly on medical surfaces.

Finally, we demonstrated that the adsorption profiles on model surfaces may not fully represent mAb and surfactant interactions on medical surfaces, emphasizing the importance of evaluating mAb adsorption directly on medical surfaces. While our research offers valuable insights into mAb and surfactant adsorption on medical surfaces, additional investigations are needed to accurately estimate mAb losses based on the material and surface area in contact with the formulation. Furthermore, exploring additional parameters such as buffer composition, pH, and diluents (*e.g.*, NaCl and Glucose 5 %) could provide deeper insights into mAb adsorption on real medical surfaces. By allowing to screen the combined material surface and formulation, our ELIBAG approach could complement existing compatibility studies (*e.g.*, in-use aggregation studies), enabling the optimization of future formulation and their compatibility at the medical surface/formulation interface.

Extensive comparative studies like this one, involving numerous model and, most importantly, in-use medical surfaces, mAb modalities and surfactant concentrations, in which the experimental protocol is rigorously identical for all tested samples, are very valuable because they overcome the invalidity issues when concluding from a compilation of smaller scale studies with dissimilar parameters and contexts. In this sense, our study allows to ascertain tendencies and extend our knowledge on the parameters crucially influencing formulation and container compatibility studies.

Moreover, the data generation of such studies, including molecular adsorption profiles for multiple therapeutic proteins and surfactants combined with data on material composition holds potential for future statistical correlation studies, paving the way towards the hitherto impossible prediction of therapeutic protein-material compatibility.

CRediT authorship contribution statement

Rosa Álvarez-Palencia Jiménez: Writing – review & editing, Writing – original draft, Methodology, Investigation, Formal analysis, Data curation. **Antoine Maze:** Data curation, Conceptualization. **Franz Bruckert:** Writing – review & editing, Validation, Supervision, Methodology, Formal analysis, Data curation, Conceptualization. **Fethi Bensaid:** Writing – review & editing, Validation, Supervision, Project administration, Investigation, Funding acquisition, Formal analysis, Conceptualization. **Naila El-Kechai:** Writing – review & editing, Validation, Supervision, Project administration, Investigation, Funding acquisition, Formal analysis, Data curation, Conceptualization. **Marianne Weidenhaupt:** Writing – review & editing, Writing – original draft, Validation, Supervision, Project administration, Methodology, Investigation, Funding acquisition, Formal analysis, Data curation, Conceptualization.

Acknowledgments

RAPJ was supported by an ANRT Cifre PhD grant (2020/1349). We acknowledge the ANR (ANR-23-CMAS-0009) for financing the IBES project. The authors thank Matthieu Weber (Univ. Grenoble Alpes, CNRS, Grenoble INP LMGP) for excellent technical expertise with XPS acquisition.

Conflicts of interest

NEK, FB, RAPJ are Sanofi employees and may hold stock and/or stock options.

Appendix A. Supplementary material

Supplementary material to this article can be found online at https://doi.org/10.1016/j.ejpb.2024.114539.

Data availability

Data will be made available on request.

References

[1] P. Hollowell, Z. Li, X. Hu, et al., Recent advances in studying interfacial adsorption of bioengineered monoclonal antibodies, Molecules 25 (9) (2020), https://doi.org/10.3390/molecules25092047.
[2] S. Crescioli, H. Kaplon, A. Chenoweth, L. Wang, J. Visweswaraiah, J.M. Reichert, Antibodies to watch in 2024, MAbs 16 (1) (2024), https://doi.org/10.1080/19420862.2023.2297450.
[3] K.P. Martin, C. Grimaldi, R. Grempler, S. Hansel, S. Kumar, Trends in industrialization of biotherapeutics: a survey of product characteristics of 89 antibody-based biotherapeutics, MAbs 15 (1) (2023), https://doi.org/10.1080/19420862.2023.2191301.
[4] T.K. Das, A. Sreedhara, J.D. Colandene, et al., Stress factors in protein drug product manufacturing and their impact on product quality, J. Pharm. Sci. 111 (4) (2022) 868–886, https://doi.org/10.1016/j.xphs.2021.09.030.
[5] C. Pinholt, R.A. Hartvig, N.J. Medlicott, L. Jorgensen, The importance of interfaces in protein drug delivery – why is protein adsorption of interest in pharmaceutical formulations? Expert Opin. Drug Deliv. 8 (7) (2011) 949–964, https://doi.org/10.1517/17425247.2011.577062.
[6] M.R.G. Kopp, F. Grigolato, D. Zürcher, et al., Surface-induced protein aggregation and particle formation in biologics: current understanding of mechanisms, detection and mitigation strategies, J. Pharm. Sci. 112 (2) (2023) 377–385, https://doi.org/10.1016/j.xphs.2022.10.009.
[7] A.D. Kanthe, M.R. Carnovale, J.S. Katz, et al., Differential surface adsorption phenomena for conventional and novel surfactants correlates with changes in interfacial mAb stabilization, Mol. Pharm. 19 (9) (2022) 3100–3113, https://doi.org/10.1021/acs.molpharmaceut.2c00152.
[8] Y. Wang, T. Wang, Q. Chen, W. Zhou, J. Guo, Correlation between the protein pharmaceutical surface activity and interfacial stability, Mol. Pharm. 20 (5) (2023) 2536–2544, https://doi.org/10.1021/acs.molpharmaceut.2c01114.
[9] S. Morar-Mitrica, M. Puri, A.B. Sassi, et al., Development of a stable low-dose aglycosylated antibody formulation to minimize protein loss during intravenous administration, MAbs 7 (4) (2015) 792–803, https://doi.org/10.1080/19420862.2015.1046664.
[10] J.S. Bee, T.W. Randolph, J.F. Carpenter, S.M. Bishop, Effects of surfaces and leachables on the stability of biopharmaceuticals, J. Pharm. Sci. 99 (5) (2010) 2386–2398, https://doi.org/10.1002/jps.
[11] Y. Le Basle, P. Chennell, N. Tokhadze, A. Astier, V. Sautou, Physicochemical stability of monoclonal antibodies: a review, J. Pharm. Sci. 109 (1) (2020) 169–190, https://doi.org/10.1016/j.xphs.2019.08.009.
[12] T.A. Khan, H.C. Mahler, R.S.K. Kishore, Key interactions of surfactants in therapeutic protein formulations: a review, Eur. J. Pharm. Biopharm. 97 (2015) 60–67, https://doi.org/10.1016/j.ejpb.2015.09.016.
[13] E.L.N. Escobar, V.P. Griffin, P. Dhar, Correlating surface activity with interface-induced aggregation in a high-concentration mAb solution, Mol. Pharm. 21 (3) (2024) 1490–1500, https://doi.org/10.1021/acs.molpharmaceut.3c01125.
[14] S.K. Singh, D.L. Luisi, R.H. Pak, Antibody-drug conjugates: design, formulation and physicochemical stability, Pharm. Res. 32 (11) (2015) 3541–3571, https://doi.org/10.1007/s11095-015-1704-4.
[15] A. Oom, M. Poggi, J. Wikström, M. Sukumar, Surface interactions of monoclonal antibodies characterized by quartz crystal microbalance with dissipation: Impact of hydrophobicity and protein self-interactions, J. Pharm. Sci. 101 (2) (2012) 519–529, https://doi.org/10.1002/jps.22771.
[16] G. Lefebvre, A. Maze, R. Alvarez-Palencia Jimenez, et al., Surfactant protection efficacy at surfaces varies with the nature of hydrophobic materials, Pharm. Res. 38 (12) (2021) 2157–2166, https://doi.org/10.1007/s11095-021-03133-6.
[17] D. Zürcher, S. Caduff, L. Aurand, U. Capasso Palmiero, K. Wuchner, P. Arosio, Comparison of the protective effect of polysorbates, poloxamer and brij on antibody stability against different interfaces, J. Pharm. Sci. 112 (11) (2023) 2853–2862, https://doi.org/10.1016/j.xphs.2023.06.004.
[18] M. Blümel, J. Liu, I. de Jong, et al., Current industry best practice on in-use stability and compatibility studies for biological products, J. Pharm. Sci. 112 (9) (2023) 2332–2346, https://doi.org/10.1016/j.xphs.2023.05.002.
[19] A. Sreedhara, Z.K. Glover, N. Piros, N. Xiao, A. Patel, B. Kabakoff, Biotechnology stability of IgG1 monoclonal antibodies in intravenous infusion bags under clinical in-use conditions, J. Pharm. Sci. 101 (1) (2012) 21–30, https://doi.org/10.1002/jps.22739.
[20] O.S. Kumru, J. Liu, J.A. Ji, et al., Compatibility, physical stability, and characterization of an IgG4 monoclonal antibody after dilution into different intravenous administration bags, J. Pharm. Sci. 101 (10) (2012) 3636–3650, https://doi.org/10.1002/jps.23224.
[21] R. Alvarez-Palencia, A. Maze, G. Vian, et al., Development of an ELISA-based device to quantify antibody adsorption directly on medical plastic surfaces, Eur. J.

Pharm. Biopharm. 203 (July) (2024), https://doi.org/10.1016/j.ejpb.2024.114425.
[22] S. Wang, G. Wu, X. Zhang, et al., Stabilizing two IgG1 monoclonal antibodies by surfactants: Balance between aggregation prevention and structure perturbation, Eur. J. Pharm. Biopharm. 114 (2017) 263–277, https://doi.org/10.1016/j.ejpb.2017.01.025.
[23] A. Kanthe, A. Ilott, M. Krause, et al., No ordinary proteins: adsorption and molecular orientation of monoclonal antibodies, Sci. Adv. 7 (35) (2021), https://doi.org/10.1126/sciadv.abg2873.
[24] V. Džupponová, G. Žoldák, Salt-dependent passive adsorption of IgG1κ-type monoclonal antibodies on hydrophobic microparticles, Biophys. Chem. 275 (2021) 1–10, https://doi.org/10.1016/j.bpc.2021.106609.
[25] S. Saurabh, Q. Zhang, Z. Li, et al., Mechanistic insights into the adsorption of monoclonal antibodies at the water/vapor interface, Mol. Pharm. 21 (2) (2024) 704–717, https://doi.org/10.1021/acs.molpharmaceut.3c00821.
[26] N. Doshi, J. Giddings, L. Luis, et al., A comprehensive assessment of all-oleate polysorbate 80: free fatty acid particle formation, interfacial protection, Pharm Res. 20 (2021) 531–548.
[27] C. Vaclaw, K. Merritt, V.P. Griffin, et al., Comparison of protein particle formation in IgG1 mAbs formulated with PS20 Vs. PS80 when subjected to interfacial dilatational stress, AAPS PharmSciTech 24 (5) (2023) 1–12, https://doi.org/10.1208/s12249-023-02561-4.
[28] W. Nicholas, H.C.M. Warne, Challenges in Protein Product Development, Vol 38. Springer, 2018. https://doi.org/10.1007/978-3-319-90603-4.
[29] M.J. Rosen, Surfactants and Interfacial Phenomena, third ed., John Wiley & Sons, Inc., 2004.
[30] R.G. Strickley, W.J. Lambert, A review of formulations of commercially available antibodies, J. Pharm. Sci. 110 (7) (2021) 2590–2608.e56, https://doi.org/10.1016/j.xphs.2021.03.017.
[31] N. Doshi, K. Rutherford, A. Najjar, Dissolution of polysorbate 20 degradation related free fatty acid particles in intravenous bag solutions, J. Pharm. Sci. 110 (2) (2021) 687–692, https://doi.org/10.1016/j.xphs.2020.10.004.
[32] S.J. Kim, K.W. Kim, Y.K. Shin, et al., In-use stability of the rituximab biosimilar CT-P10 (Truxima®) following preparation for intravenous infusion and storage, BioDrugs 33 (2) (2019) 221–228, https://doi.org/10.1007/s40259-019-00336-7.
[33] I. Krämer, J. Thiesen, A. Astier, Formulation and administration of biological medicinal products, Pharm. Res. 37 (8) (2020), https://doi.org/10.1007/s11095-020-02859-z.
[34] V. Linkuvienė, E.L. Ross, L. Crawford, et al., Effects of transportation of IV bags containing protein formulations via hospital pneumatic tube system: particle characterization by multiple methods, J. Pharm. Sci. 111 (4) (2022) 1024–1039, https://doi.org/10.1016/j.xphs.2022.01.016.
[35] J.R. Snell, C.R. Monticello, C. Her, et al., DEHP nanodroplets leached from polyvinyl chloride IV bags promote aggregation of IVIG and activate complement in human serum, J. Pharm. Sci. 109 (1) (2020) 429–442, https://doi.org/10.1016/j.xphs.2019.06.015.
[36] M. Wozniewski, A. Besheer, A.S. Sediq, J. Huwyler, H.C. Mahler, V. Levet, Characterization of silicone from closed system transfer devices and its migration into pharmaceutical drug products, J. Pharm. Sci. 113 (2) (2024) 419–426, https://doi.org/10.1016/j.xphs.2023.11.012.
[37] H. Al Salloum, J. Saunier, A. Dazzi, et al., Characterization of the surface physico-chemistry of plasticized PVC used in blood bag and infusion tubing, Mater. Sci. Eng. C 75 (2017) 317–334, https://doi.org/10.1016/j.msec.2017.02.057.